Int. J. Heat Mass Transfer. Vol. 25, No. 10, pp. 1461–1467, 1982
Printed in Great Britain

0017-9310/82/101461-07 $03.00/0
Pergamon Press Ltd.

HEAT AND MASS TRANSFER WITHIN AN INTENSELY HEATED CONCRETE SLAB

ABRAHAM DAYAN
University of Tel-Aviv, Tel-Aviv, Israel

and

EMIL L. GLUEKLER
General Electric Company, Sunnyvale, CA 94086, U.S.A.

(*Received* 2 *November* 1981)

Abstract—A model for the heat and mass transfer within a surface heated concrete slab has been developed. The concrete is treated as a porous material containing water, vapor and air. The solution of the problem for various temperature and heat flux boundary conditions has been obtained with an explicit numerical scheme. The results consist of temperature, pore pressure and moisture distributions as a function of time. The rate of steam release from the drying concrete is also calculated. The code predictions were successfully tested with preliminary experimental data. The results demonstrate the importance of the evaporation–recondensation mechanism in enhancing the rate of heat transfer.

NOMENCLATURE

c, specific heat at constant volume;
c_p, specific heat at constant pressure;
D, mass diffusivity;
e, specific energy;
h, specific enthalpy;
j, mass diffusion flux;
k, permeability;
K, thermal conductivity;
P, pressure;
R_i, gas constant of the ith species;
S, pore volume fraction occupied by gas;
t, time;
T_a, absolute temperature;
T, temperature;
u, superficial velocity;
u_{fg}, specific energy of vaporization at constant volume;
V_i, functions defined by equations (10)–(13);
x, distance from heated surface.

Greek symbols

ε, porosity;
μ, viscosity;
ρ, density;
ω, mass fraction.

Subscripts

0, dry concrete;
1, liquid moisture;
2, water vapor;
3, air;
d, dry;
g, gas;
w, wet.

INTRODUCTION

SURFACE heating of concrete to elevated temperatures results in significant heat release by evaporation of water held within the porous structure in form of capillary, adsorbed and chemically bound water. The release of steam degrades the concrete strength and can under some conditions affect the surrounding through pressurization and chemical reaction. Evaluations of steam release rates from concrete as well as thermal response to heating have important applications in safety assessments of nuclear reactors and, more generally, assessments of structural damage in buildings caused by fires. The applicability of the present solution extends to a wider spectrum of engineering problems involving multiphase, multicomponent heat and mass transfer in porous media.

Moisture migration within heated concrete was first regarded as a mass diffusion process [1]. However, this theory could not explain observed migration into areas of high moisture concentration. Therefore, moisture transport was attributed also to thermal diffusion (Soret effect) [2]. Experiments conducted at elevated temperatures (higher than 105°C) revealed that filtration (pressure driven flow) becomes the dominant transport mechanism [3–5]. Heating of the concrete results in the evaporation of water and subsequent pressurization of both vapor and air within the pores. The migration that follows this pressurization leads to releases of vapor from the structure boundaries. Sustained heating of one of the surfaces provides continuous evaporation and drying of the region near the surface. In deeper region, the concrete remains wet and actually gains moisture from recondensation. The dry–wet interface or evaporation front that separates the two regions penetrates into the structure with further evaporation [4].

Early studies on the drying of porous media were based on principles of irreversible thermodynamics [6–9]. Being mainly concerned with low temperature drying, pressure terms in the governing equations were neglected. Later, these terms were included in studies on low temperature drying of clay bricks [10] and concrete [11, 12]. In these investigations it was assumed that moisture migration takes place predominantly in the gaseous phase and that sorption curves are adequate to describe the equilibrium moisture content. The evaporation–recondensation mechanism was found to play a major role in the drying process.

At elevated temperatures the important mass transport mechanisms are those resulting from pressure and concentration gradients. Indirect modes of transport, such as the Soret and Dufour effects, can be neglected. In the modeling of drying of a moist porous structure, generally, a clear distinction between dry and wet zones can be made. To calculate maximal pressure buildup or the location of the dry–wet interface, some investigators simplified the problem by neglecting the convection terms in the energy equation [13, 14]. Others only neglected the mass diffusion terms [15, 16]. To determine the drying characteristics of weakly wetted packed aluminum oxide powder, a simplified solution of the equations, including filtration and diffusion, was obtained by linearization of the dry zone pressure profile [17].

The evaporation–recondensation model was applied in two separate investigations to study the drying of concrete. In one, an implicit numerical scheme was used to obtain a solution for equations in which lower order terms were neglected and material properties were essentially constant [18]. In the other, conducted by the authors, an explicit scheme was utilized to solve the equations which included terms for liquid moisture filtration and moisture dependent material properties [19–21]. This model was successfully tested with limited experimental data obtained elsewhere [22]. The purpose of this paper is to present the model and its supporting test data. It should be noted that the experimental data on pressure and moisture distribution within intensely heated concrete are very limited. These quantities are quite difficult to measure [4, 23]. More data, however, exist on temperature distributions [24].

MATHEMATICAL MODEL

Consider a planar concrete slab consisting of hydrated cement paste with no aggregate. The solid gel contains capillaries and gel pores in which evaporable water exists. The moisture content in the pores depends on both temperature and relative humidity [25]. Following intense heating of one of the concrete surfaces, a region near the heated surface dries out. Once such a region develops, evaporation takes place exclusively at the dry–wet zone interface [17]. The evaporation process leads to pore pressurization and subsequent filtration of all pore constituents towards both the heated surface and the inner wet zone of the concrete. In general, the transport of the gaseous species occurs under pressure and concentration gradients. The migration of the liquid phase is primarily governed by pressure gradients. Local thermodynamic equilibrium can be assumed to exist between vapor and liquid in the wet region. Under sustained surface heating, the dry zone advances into the concrete (Fig. 1).

The conservation equation for mass and energy are written for the dry and wet zone separately. In the dry zone the continuity and energy equations are, respectively,

$$\varepsilon \frac{\partial \rho_i}{\partial t} + \frac{\partial}{\partial x}(u_g \rho_i + j_i) = 0 \quad i = 2, 3 \tag{1}$$

$$(1-\varepsilon)\rho_0 \frac{\partial e_0}{\partial t} + \sum_{i=2}^{3}\left[\varepsilon \frac{\partial(\rho_i e_i)}{\partial t} + \frac{\partial}{\partial x}(u_g \rho_i + j_i)h_i\right] = K_d \frac{\partial^2 T}{\partial x^2} \tag{2}$$

where ε denotes the porosity, ρ_2 and ρ_3 the density of vapor and air, t the time, u_g the volumetric flow rate of gases in the x direction per unit area, j_i the diffusive mass flux of the ith species, ρ_0 the density of the solid phase, e the specific internal energy, h the specific enthalpy, K_d the thermal conductivity of the dry zone, and T the temperature in °C. Likewise the species equations for the wet region are

$$\varepsilon \frac{\partial}{\partial t}\left[(1-S)\rho_1 + S\rho_2\right] + \frac{\partial}{\partial x}(u_1\rho_1 + u_g\rho_2 + j_2) = 0 \tag{3}$$

$$\varepsilon \frac{\partial}{\partial t}(S\rho_3) + \frac{\partial}{\partial x}(u_g\rho_3 + j_3) = 0 \tag{4}$$

and the energy equation for the wet region is

$$(1-\varepsilon)\rho_0 \frac{\partial e_0}{\partial t} + \varepsilon \frac{\partial}{\partial t}[(1-S)\rho_1 e_1 + S(\rho_2 e_2 + \rho_3 e_3)] + \frac{\partial}{\partial x}[u_1\rho_1 h_1 + (u_g\rho_2 + j_2)h_2 + (u_g\rho_3 + j_3)h_3] = K_w \frac{\partial^2 T}{\partial x^2} \tag{5}$$

in which S designates the volume fraction of the pores occupied by gases, ρ_1 the liquid density, u_1 the liquid apparent velocity, e_1 and h_1 the liquid specific energy and enthalpy, respectively. The filtration velocity of the gas phase is determined according to Darcy's law,

$$u = -\frac{k(S)}{\mu}\frac{\partial P}{\partial x} \tag{6}$$

in which P denotes pore pressure and μ viscosity. The permeability $k(S)$ is assumed to be directly proportional to the gas volume fraction within the pores, $k(S) = k_d S$ (k_d is the permeability of dry concrete). This

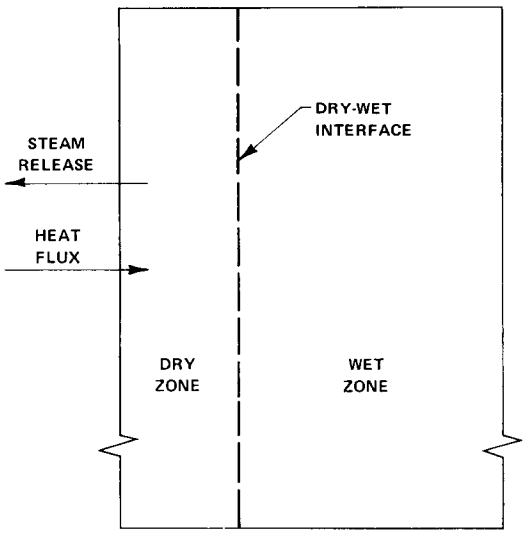

FIG. 1. Physical model of a heated concrete slab.

relationship reasonably approximates measured permeabilities of porous ceramic materials [10]. The liquid velocity u_1 is determined from the same law, but the liquid permeability, k_1 which is usually smaller than the permeability of gas, is assumed to be moisture independent. The diffusive flux of the ith gaseous species is given by Fick's law

$$j_i = -\rho D(S)\frac{\partial \omega_i}{\partial x} \tag{7}$$

where ρ is the air–vapor mixture density, ω_i the mass fraction of the ith species and $D(S)$ the moisture dependent coefficient, $D(S) = D_d \cdot S$ (D_d is the diffusion coefficient of dry concrete). Since the liquid velocity is much smaller than the gas velocity, the presence of the liquid can be regarded as a reduced porosity equal to εS. Thus the diffusion coefficient, which is approximately proportional to the porosity, becomes proportional to the volume fraction of the pore occupied by gas.

Air and water vapor are assumed to behave like an ideal binary mixture which obeys Dalton's law, i.e.

$$\begin{aligned} P_i &= \rho_i R_i T_a \\ e_i &= c_i T \\ h_i &= c_{pi} T \\ P &= P_2 + P_3 \end{aligned} \tag{8}$$

where R_i is the gas constant of the ith species, T_a the absolute temperature in degrees Kelvin, c and c_p are the specific heat at constant volume and at constant pressure, respectively. The water density and specific heats are assumed constant. Since the zero energy reference is assigned to the vapor at 0°C, the specific energy of water is $u_1 = -u_{fg} + c_1 T$, where u_{fg} is the specific heat of vaporization at constant volume. In the wet region, water is assumed to be in equilibrium with its liquid phase [3]. This assumption is justified in view of the enormous specific surface of the concrete porous structure ($2 \times 10^5\ m^2\ kg^{-1}$) and its low permeability [26]. Under equilibrium conditions, the vapor pressure is a function of temperature only. The temperature–pressure dependence was obtained from integration of the Clausius–Clapeyron equation

$$P = 1.055 \times 10^{21}\, T_a^{-5} \exp(-7000/T_a) \qquad (273\,K < T_a < 450\,K) \tag{9}$$

where the pressure is in atmospheres.

In addition to the above equation it is understood that continuity of energy and mass fluxes at the dry–wet interface exists. The solution method, however, does not require the explicit formulation of these conditions.

SOLUTION METHOD

An explicit numerical scheme was developed to solve the governing equation subject to arbitrary initial and boundary conditions. The slab was subdivided into a finite number of equally spaced nodal points. The dry–wet interface was assumed to be located right in between the dry and wet nodal points. With this approach, the interface remains stationary as long as the wet node next to the interface has not reached dry out. When local dry out is reached, by definition, the dry–wet interface relocates to separate the next two nodes. The sudden jumps of the interface produce some fluctuations in the pressure response since pressure depends on local temperatures in the wet region. These fluctuations can be reduced by decreasing the grid size.

The governing equations of the dry region are in a form readily suitable for discretization and explicit representation of density and temperature variations with time. The divergence terms of equation (1) yield the densities time derivatives. These derivatives and the divergence terms of equation (2) give the temperature time derivative. Knowing the time derivatives permits calculation of new properties distributions based on known distributions at a previous time step.

The wet region contains one additional variable when compared to the dry region. This is the volume fraction of the pores occupied by vapor. Equations (3), (4) and (5) contain the time derivative of this variable in addition to others. Therefore, it was necessary to calculate first the time derivative of S in order to proceed with the computation of all other parameters with the same routine used for the dry region. The choice of computing S first also allowed an early check on the position of the dry–wet interface. If after a time increment the value of S in the wet node adjacent to the interface becomes unity or more, it implies that sometime during the time incremental the node has dried out by becoming vapor saturated. A value of S greater than unity, indicates that the moisture flux out of the grid was sufficient to expell more moisture than it contained during the full time interval. In such a case

it is necessary to proportionately reduce the time incremental to one which yields an exact dry out, i.e. $S = 1$.

In order to calculate the time derivative of the vapor saturation parameter S the following definitions were made:

$$V_1 = \frac{\partial}{\partial x}(u_l\rho_l + u_g\rho_2 + j_2), \tag{10}$$

$$V_2 = \frac{\partial}{\partial x}(u_g\rho_3 + j_3), \tag{11}$$

$$V_3 = \frac{\partial}{\partial x}\left[u_l\rho_l h_l + (u_g\rho_2 + j_2)h_2 + (u_g\rho_3 + j_3)h_3 - K_w\frac{\partial T}{\partial x}\right] \tag{12}$$

and

$$V_4 = c_2 T + [(1-\varepsilon)\rho_0 c_0 + \varepsilon\rho_l c_l(1-S) + \varepsilon S(\rho_2 c_2 + \rho_3 c_3)]\Big/\left(\varepsilon S\frac{\partial\rho_2}{\partial T}\right). \tag{13}$$

The first three definitions represent divergences of fluxes. The expression in the square brackets of equation (13) designates the volumetric heat capacity of the concrete and its constituents. The vapor density temperature derivative was obtained from the saturation density–temperature relationship. According to equation (9) and the ideal gas law this relationship is

$$\rho_2 = 1.055 \times 10^{21}\, T_a^{-6} R_2^{-1} \exp(-7000/T_a). \tag{14}$$

The temperature time derivatives of equation (5) were converted to vapor density derivatives by incorporating equation (14) and

$$\frac{\partial\rho_2}{\partial t} = \frac{\partial\rho_2}{\partial T}\frac{\partial T}{\partial t}. \tag{15}$$

The densities time derivatives from equations (3) and (4) were then substituted in equation (5) to obtain the time derivative of S

$$\frac{\partial S}{\partial t} = \frac{1}{\varepsilon}\left[\frac{V_1 V_4 + c_3 T V_2 - V_3}{V_4(\rho_l - \rho_2) + \rho_l u_{fg} + (\rho_2 c_2 - \rho_l c_l)T}\right]. \tag{16}$$

The stability of the numerical calculations was assured by using three stability criteria for time incrementals. The first two are those of the heat conduction and mass diffusion mechanisms which are, respectively,

$$\Delta t \leqslant \frac{(1-\varepsilon)\rho_0 c_0 \Delta x^2}{2K_w} \tag{17}$$

and

$$\Delta t \leqslant \frac{\varepsilon\Delta x^2}{2D} \tag{18}$$

where Δt is the time incremental, Δx the grid size and c_0 the specific heat of solid structure. Criteria (17) and (18) are not time dependent and are calculated once for each run. The third criterion is for the filtration mechanism and is

$$\Delta t \leqslant \frac{\varepsilon\mu}{2k}\frac{\Delta x^2}{P_{max}}. \tag{19}$$

The maximum pore pressure in the structure changes continuously. Therefore, criterion (19) must be checked for each time increment.

Table 1. Material properties used in the test analysis

Symbol	Value	Dimensions
ρ_0	2500	kg m^{-3}
ρ_l	1000	kg m^{-3}
c_0	1000	J kg^{-1} °C^{-1}
c_{pl}	4200	J kg^{-1} °C^{-1}
c_{p2}	2016	J kg^{-1} °C^{-1}
c_{p3}	1050	J kg^{-1} °C^{-1}
ε	0.32	None
K_d	0.35	W m^{-1} °C^{-1}
K_w	1.6	W m^{-1} °C^{-1}
k/μ	2.4×10^{-6}	m^2 atm^{-1} s^{-1}
$(k/\mu)_{liquid}$	2.4×10^{-10}	m^2 atm^{-1} s^{-1}
D_d	10^{-6}	m^2 s^{-1}

RESULTS

The developed numerical code was used to analyze experimental data on concrete dehydration [22]. In the experiment, a cylindrical concrete slab, 0.6 m dia. and 0.3 m thick, was heated by a steel plate on one side and maintained at room temperature on the other side. Temperatures and pressures were recorded at several axial locations. Vapor released from the concrete was collected and weighed at various times.

The test program also included some measurements of concrete permeability. Other material properties

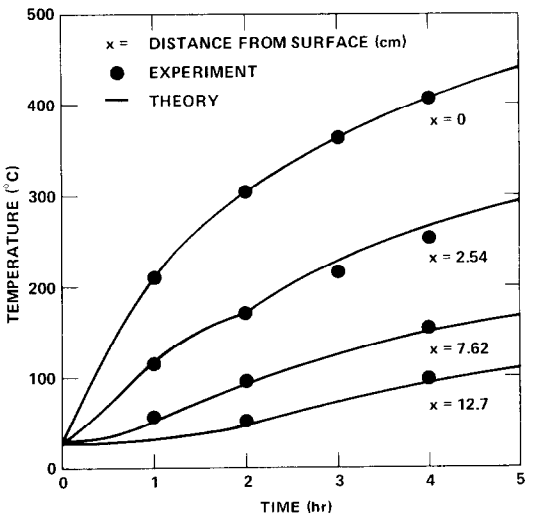

FIG. 2. Thermal response of a heated concrete slab.

were obtained from the open literature [25, 26, 27]. Their values are listed in Table 1. The initial moisture content was not reported and had to be retrieved from the test results (initially $S = 0.18$). It is important to note that the concrete used in the test was not fully aged and contained magnetite aggregate (with a mixing ratio of 5:1). The aging of 47 days could hydrate only 85% of the cement [25]. The porosity of the hydrated gel is 0.26 [25]. In addition, the specimens contained capillary pores which depend on the water–cement mixing ratio and the degree of hydration. Since the water–cement mixing ratio of the test specimen was 0.5 it produced capillary pores [22, 25]. An overall porosity of 0.32 was calculated (assuming that the aggregate porosity is 0.32). Moisture within the concrete was found high since it was cured in a moist environment.

The concrete surface temperature was recorded by a thermocouple. This was used as a prescribed boundary condition in the analysis. Atmospheric pressure of dry air was assumed to exist near the concrete surface. A comparison of measured and calculated temperature responses at 2.56, 7.62 and 12.7 cm from the heated surface is shown in Fig. 2. The sudden change in the rate of temperature rise at 2 h at a depth of 2.54 cm indicates that at this time the dry–wet interface reached this location. The pressure response at a depth of 2.54 cm is illustrated in Fig. 3. It can be concluded that a peak pressure exists at the dry–wet interface. Measured pressure responses at other locations were meaningless because of apparent crack formations. This trend of pressure rise and decrease was seen also in another investigation [18]. The pressure response indicated in [18] for the appropriate boundary conditions have been reproduced with the present code. Predicted and measured data on time averaged water release rates are shown in Fig. 4. In general, experimental and predicted results were found to be in good

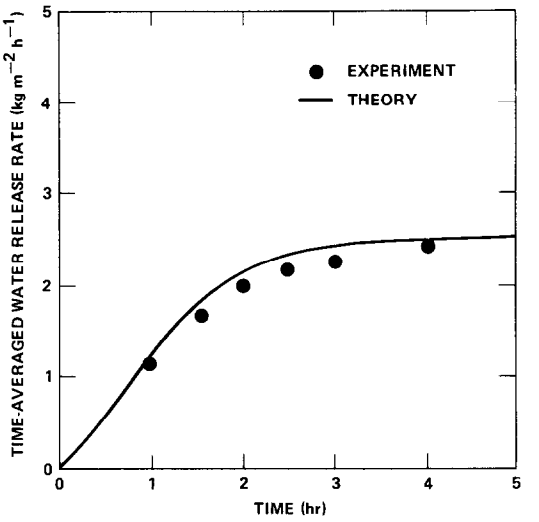

FIG. 4. Time-averaged water release rate from a heated concrete slab.

agreement. Small discrepancies are well within the accuracy expected from concrete modelling.

Spatial distributions of temperature, pressure and moisture content in pores are plotted in Figs. 5 and 6. The points of discontinuity, in temperature gradients (Fig. 5) represent the momentary locations of the dry–wet interface. The reduced temperature gradient near the interface and in the adjacent wet zone is produced by the enhanced heat transfer owing to both a higher thermal conductivity and the evaporation–recondensation mechanism. The moisture distributions (Fig. 5) indicate that a high moisture concentration exists near the interface. Fig. 6 shows that the peak pore pressures exist near the interface. Therefore, if such peak pressures were sufficient to crack the concrete, one would expect to find wet fracture surfaces. Indeed, these have been observed

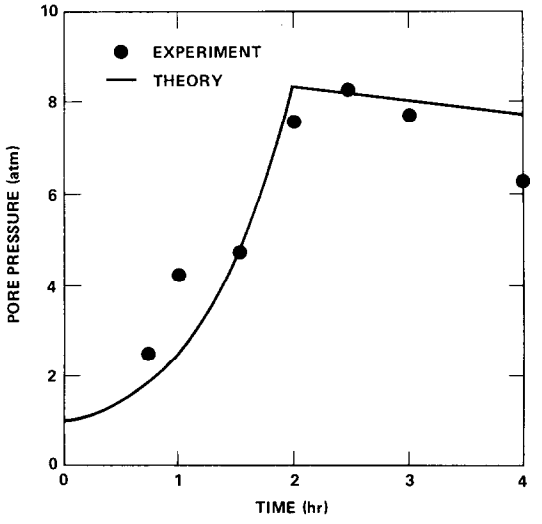

FIG. 3. Pressure response within a heated concrete slab at a depth of 2.54 cm from the heated surface.

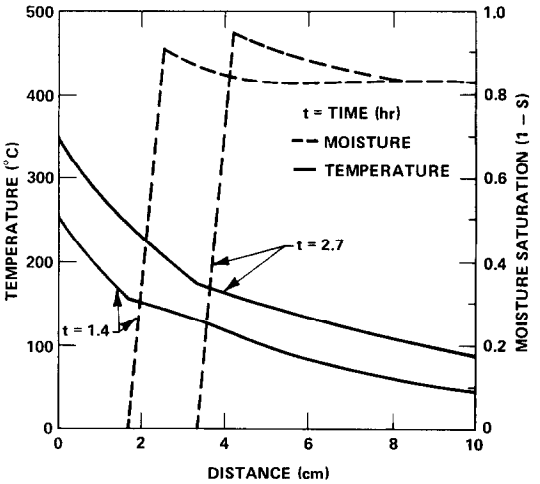

FIG. 5. Distributions of temperature and pore saturation with evaporable moisture within a heated concrete slab.

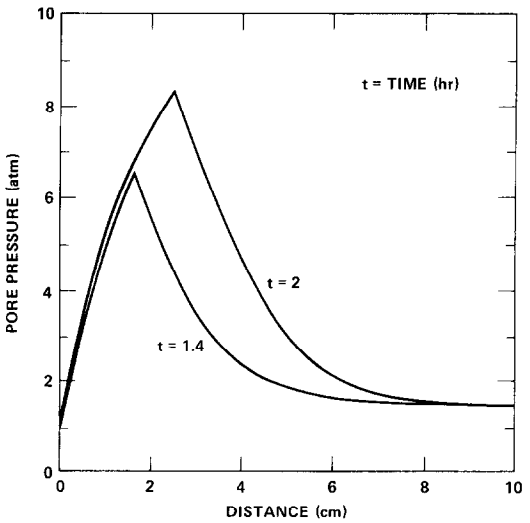

FIG. 6. Pore pressure distribution within a heated concrete slab.

in experiments [24]. Concrete interactions with hot metals can lead to concrete spallation and exposure of totally wet fracture surfaces. The shape of the moisture distribution near the dry–wet interface as shown in Fig. 5 is approximated. To obtain a more precise shape one must know the exact position of the interface. Furthermore, the width of the interface region is expected to expand with reduced heating rates owing to increased importance of capillary forces and concrete inhomogeneity effects of the structure irregularities which tend to diminish sharp moisture gradients. To the right of the interface, a gain of moisture can be observed. The augmented moisture content results from both vapor recondensation and liquid filtration. Similar moisture distribution characteristics were obtained experimentally [4, 23].

CONCLUSIONS

The model developed for the heat and mass transport within heated concrete was successfully tested with initial experimental results. Results obtained with the model exhibit many characteristics observed in experiments and related theoretical investigations. The model has been successfully applied to conduct studies on water release from heated concrete structures in support of fast breeder reactor safety analyses. Efforts have been made to extend its range of applicability to higher temperatures (350°C), where non-evaporable water is released following the decomposition of the solid material. The supplemental version of the code has not yet been verified and therefore was not presented. There is a need for more experimental work especially in the measurement of pore pressure distribution, moisture distribution and material properties of both cement and aggregate.

REFERENCES

1. R. L. Yuan, H. K. Hilsdorf and C. E. Kesler, The effect of temperature on the drying of concrete, in *Concrete for Nuclear Reactors*, Vol. 2, American Concrete Institute Spec. Publ. No. 34, pp. 991–1019 (1972).
2. S. E. Pihlajavara and K. Tinsanen, A preliminary study of thermal moisture transfer in concrete, in *Concrete for Nuclear Reactors*, Vol. 2, American Concrete Institute Spec. Publ. No. 34, pp. 1019–1033 (1972).
3. G. L. England and T. J. Sharp, Migration of moisture and pore pressures in heated concrete, *Proc. 1st Int. Conf. on Structural Mechanics in Reactor Technol.*, H 2/4, pp. 129–143 (1971).
4. D. A. Chapman and G. L. England, Effects of moisture migration on shrinkage, pore pressure and other concrete properties, *Trans. 4th Int. Conf. on Structural Mechanics in Reactor Technol.*, H 5/3, pp. 1–14 (1977).
5. Z. P. Bazant, Some questions of material inelasticity and failure in the design of concrete structures for nuclear reactors, *Trans. 3rd Int. Conf. on Structural Mechanics in Reactor Technol.*, H 1/1*, pp. 1–11 (1975).
6. L. N. Gupta, An approximate solution of the generalized Stefan's problem in a porous medium, *Int. J. Heat Mass Transfer* **17**, 313–321 (1974).
7. S. H. Cho, An exact solution of the coupled phase change problem in a porous medium, *Int. J. Heat Mass Transfer* **18**, 1139–1142 (1975).
8. M. D. Mikhailov and B. K. Shishedjiev, Temperature and moisture distributions during contact drying of moist porous sheet, *Int. J. Heat Mass Transfer* **18**, 15–24 (1975).
9. M. D. Mikhailov, Exact solution of temperature and moisture distributions in a porous half-space with moving evaporation front, *Int. J. Heat Mass Transfer* **18**, 797–804 (1975).
10. T. Z. Harmathy, Simultaneous moisture and heat transfer in porous systems with particular reference to drying, *I/EC Fundamentals* **8**, 92–103 (1969).
11. C. L. D. Huang, H. H. Siang and C. H. Best, Heat and moisture transfer in concrete slab, *Int. J. Heat Mass Transfer* **22**, 252–266 (1979).
12. C. L. D. Huang, Multi-phase moisture transfer in porous media subjected to temperature gradient, *Int. J. Heat Mass Transfer* **22**, 1295–1307 (1979).
13. M. Cross, R. D. Gibson and R. W. Young, Pressure generation during the drying of a porous half-space, *Int. J. Heat Mass Transfer* **22**, 47–50 (1979).
14. R. D. Gibson, M. Cross and R. W. Young, Pressure gradients generated during the drying of porous shapes, *Int. J. Heat Mass Transfer* **22**, 827–830 (1979).
15. F. A. Morrison, Transient multiphase multicomponent flow in porous media, *Int. J. Heat Mass Transfer* **16**, 2331–2342 (1973).
16. H. Saito and N. Seki, Mass transfer and pressure rise in moist porous material subjected to sudden heating, *Trans. Am. Soc. Mech. Engrs*, Series C, *J. Heat Transfer* **99**, 105–112 (1977).
17. K. Min and H. W. Emmons, The drying of porous media, *Proc. 1972 Heat Transfer and Fluid Mech. Inst.* pp. 1–18., Stanford University Press (1972).
18. M. S. Sahota and P. J. Pagni, Heat and mass transfer in porous media subject to fires, *Int. J. Heat Mass Transfer* **22**, 1069–1081 (1979).
19. E. L. Gluekler and A. Dayan, Considerations of the third line of assurance, post-accident heat removal and core retention in containment, *Proc. Int. Meeting Fast Reactor Safety and Related Physics*. USERDA Publication, CONF-761001, Vol. 4, pp. 1995–2004 (1976).
20. A. Dayan and E. L. Gluekler, Heat and mass transfer behind a heated reactor cell liner, *Trans. Am. Nucl. Soc.* **26**, 401–402 (1977).
21. E. L. Gluekler, A. Dayan, F. Hayes and C. T. Kline, Transient containment response and inherent retention

capability, *Int. J. Nucl. Engng Des.* **42**, 151–167 (1977).
22. J. D. McCormack, A. K. Postma and J. A. Schur, Water evolution from heated concrete, Hanford Engineering Development Laboratory, HEDL Report No. TME 78-87/UC-79 H,P (1979).
23. A. Zelinger and R. Hubner, Measurement of moisture motion under a temperature gradient in a concrete for SNR-300 using thermal neutrons, *Trans. 3rd Int. Conf. on Structural Mechanics in Reactor Technol.*, H 1/9, pp. 1–11 (1975).
24. F. B. Cheung, L. Baker and J. D. Bingle, Diffusion of heat in concrete at elevated temperatures, ASME Publication No. 76-WA/HT-79 (1976).
25. H. Hilsdorf, The water content of hardened concrete, University of Illinois Report No. DASA-1875, Urbana (1967).
26. A. M. Neville, *Properties of Concrete*. John Wiley, New York (1973).
27. D. K. Edwards, V. E. Denny and A. F. Mills, *Transfer Processes*. Hemisphere, New York (1979).
28. E. L. Gluekler and A. Dayan, Concrete failure modes at elevated temperatures, *Proc. 3rd post-accident heat removal* "Information exchange", Argonne National Laboratory Publication No. ANL-78-10, Argonne (1977).

TRANSFERT DE CHALEUR ET DE MASSE DANS UNE PLAQUE DE BETON FORTEMENT CHAUFFEE

Résumé—On développe un modèle pour le transfert de chaleur et de masse dans une plaque de béton chauffée en surface. Le béton est traité comme un matériau poreux contenant de l'eau, de la vapeur d'eau et de l'air. La solution du problème pour différentes conditions aux limites de température et de flux est obtenues avec un schéma numérique explicite. Les résultats donnent les distributions de température, de pression et d'humidité en fonction du temps. Le débit de vapeur dégagé du béton est calculé. Les précisions du code sont favorablement confrontées aux données expérimentales préliminaires. Les résultats montrent l'importance du mécanisme d'évaporation—recondensation dans l'accroissement du transfert thermique.

WÄRME- UND STOFFTRANSPORT IN EINER STARK GEHEIZTEN BETONPLATTE

Zusammenfassung—Es wurde ein Modell für den Wärme- und Stofftransport in einer an der Oberfläche beheizten Betonplatte entwickelt. Der Beton wird als poröses Material betrachtet, welches Wasser, Wasserdampf und Luft enthält. Die Lösung des Problems für verschiedene Randbedingungen der Temperatur und Wärmestromdichte wurde mittels eines expliziten numerischen Verfahrens erhalten. Die Ergebnisse sind Temperatur, Porendruck und Feuchtigkeitsverteilung als Funktion der Zeit. Der Dampfstrom aus dem trocknenden Beton wird auch berechnet. Die Gültigkeit der Rechenergebnisse wurde erfolgreich mit experimentellen Daten einer Voruntersuchung überprüft. Die Ergebnisse zeigen die Bedeutung des Verdampfungs-Rekondensations-Mechanismus für die Erhöhung des Wärmeübergangs.

ТЕПЛО- И МАССОПЕРЕНОС В ИНТЕНСИВНО НАГРЕВАЕМОЙ БЕТОННОЙ ПЛИТЕ

Аннотация — Разработана модель тепло- и массопереноса в нагреваемой с поверхности бетонной плите. Бетон рассматривается как пористый материал, содержащий воду, водяной пар и воздух. С использованием явной численной схемы дано решение задачи для различных температур и тепловых потоков на границе. Получена зависимость распределений температуры, давления в порах и влажности от времени. Проведен также расчет скорости выделения пара при сушке бетона. Результаты расчета хорошо согласуются с предварительно полученными экспериментальными данными. Показана важность механизма испарения и переконденсации в интенсификации теплопереноса.